Cell

Selective Anchoring of TFIID to Nucleosomes by Trimethylation of Histone H3 Lysine 4

Michiel Vermeulen,[1] Klaas W. Mulder,[2,4] Sergei Denissov,[3,4] W.W.M.Pim Pijnappel,[2,4] Frederik M.A. van Schaik,[2] Radhika A. Varier,[2] Marijke P.A. Baltissen,[2] Henk G. Stunnenberg,[3] Matthias Mann,[1,5,*] and H.Th.Marc Timmers[2,5,*]

[1]Department of Proteomics and Signal Transduction, Max-Planck-Institute for Biochemistry, D-82152 Martinsried, Germany
[2]Department of Physiological Chemistry, University Medical Centre-Utrecht, Universiteitsweg 100, 3584 CG Utrecht, The Netherlands
[3]Department of Molecular Biology, Nijmegen Centre for Molecular Life Sciences, Radboud University, 6500 HB Nijmegen, The Netherlands
[4]These authors contributed equally to this work.
[5]These authors contributed equally to this work.
*Correspondence: mmann@biochem.mpg.de (M.M.), h.t.m.timmers@umcutrecht.nl (H.Th.M.T.)
DOI 10.1016/j.cell.2007.08.016

SUMMARY

Trimethylation of histone H3 at lysine 4 (H3K4me3) is regarded as a hallmark of active human promoters, but it remains unclear how this posttranslational modification links to transcriptional activation. Using a stable *i*sotope *l*abeling by *a*mino acids in *c*ell culture (SILAC)-based proteomic screening we show that the basal transcription factor TFIID directly binds to the H3K4me3 mark via the plant homeodomain (PHD) finger of TAF3. Selective loss of H3K4me3 reduces transcription from and TFIID binding to a subset of promoters in vivo. Equilibrium binding assays and competition experiments show that the TAF3 PHD finger is highly selective for H3K4me3. In transient assays, TAF3 can act as a transcriptional coactivator in a PHD finger-dependent manner. Interestingly, asymmetric dimethylation of H3R2 selectively inhibits TFIID binding to H3K4me3, whereas acetylation of H3K9 and H3K14 potentiates TFIID interaction. Our experiments reveal crosstalk between histone modifications and the transcription factor TFIID. This has important implications for regulation of RNA polymerase II-mediated transcription in higher eukaryotes.

INTRODUCTION

The organization and functional state of chromatin is closely linked to posttranslational modifications of histones (Jenuwein and Allis, 2001). Histone modification patterns are involved in processes determining cell fate, development, and carcinogenesis (Carrozza et al., 2003; Margueron et al., 2005; Santos-Rosa et al., 2002; Torres-Padilla et al., 2007). Modified histones are thought to serve as binding scaffolds for regulatory proteins that translate these modifications into physiological responses. Genome-wide localization studies show that trimethylation of histone H3K4 (H3K4me3) marks active promoters in human cells in a pattern very similar to H3K9 and K14 acetylation (Bernstein et al., 2005; Heintzman et al., 2007). Recently, several interactors of methylated H3K4 have been identified. These interactors bind to methylated H3K4 via different domains, such as WD-40, Tudor, MBT, and the plant homeodomain (PHD) (Kim et al., 2006; Ruthenburg et al., 2007).

The genome-wide distributions of H3K4me3 and H3K9,14Ac are highly similar to that of the human TAF1 protein (Bernstein et al., 2005; Heintzman et al., 2007), which represents the largest subunit of TFIID. Promoter recruitment of this basal transcription factor is stimulated by gene-specific transcription factors and transcriptional cofactors. Besides TAF1, TFIID harbors TATA-binding protein (TBP) in association with 12–13 additional TBP-associated factors (Tora, 2002). In addition to histone-fold motifs, which are important for TAF-TAF interactions within TFIID (Leurent et al., 2004 and references therein), several other conserved motifs (HMG, NHR1, DUF1546, LisH, WD-40, PHD) have been identified. The relevance of these domains, if any, for promoter activation is not clear yet. In contrast, the double bromodomain of metazoan TAF1 has been shown to preferentially bind diacetylated histone H4 peptides and with a lower affinity also binds monoacetylated peptides (Jacobson et al., 2000). To summarize, while it is clear that histone acetylation and methylation cooperate in the activation of promoters, the crosstalk between these modifications at the level of the basal transcription machinery has not been explored fully.

Mass spectrometry (MS)-based proteomics has become a powerful tool in biology and for identification of histone modifications, in particular (Aebersold and Mann, 2003; Taverna et al., 2007). We have previously used quantitative proteomics to dissect regulatory pathways (Mann, 2006; Olsen et al., 2006; Ong and Mann, 2005). Here we employ a screen to identify peptide-protein interactions by *s*table *i*sotope *l*abeling by *a*mino acids in *c*ell culture (SILAC) (Schulze and Mann, 2004). In addition to several known interaction partners for H3K4me3, we unexpectedly identified subunits of the basal transcription factor TFIID as specific binders. We show that H3K4me3 binding is mediated by the PHD finger of the TAF3 subunit and that the methylation mark is essential for this PHD to bind native nucleosomes in vitro and in vivo. Overexpression of TAF3 can enhance transcription stimulation by the Ash2L subunit of Set1/MLL (mixed-lineage leukemia) histone methyltransferases in a PHD-dependent manner. Furthermore, we demonstrate that asymmetric dimethylation of H3R2 can selectively inhibit, and that acetylation of H3K9 and H3K14 potentiates, TFIID interaction with the K4-methylated H3 tail. These experiments reveal a direct connection between the basal transcription apparatus and transcriptionally active chromatin and expand our view of how histone modifications support transcriptional activation by TFIID.

RESULTS

TFIID Binds to Trimethylated Histone H3 Lysine 4 In Vitro and In Vivo

In order to identify novel proteins interacting with H3K4me3, we set up a peptide pull-down approach making use of the SILAC technology. In SILAC, one or more amino acids are replaced with their stable isotope-labeled counterpart, thus generating "light"- and "heavy"-labeled proteins, which are distinguishable and quantifiable by MS. The experimental approach for identification of interaction partners of modified histones is depicted in Figure 1A. Nuclear extracts derived from human HeLaS3 cells grown in light or heavy medium are incubated with immobilized histone peptides in the nonmethylated and methylated form, respectively. After incubation and extensive washing, beads from both pull-downs are pooled, boiled in loading buffer, and run on an SDS-PAGE gel. Following in-gel trypsin digestion and peptide extraction, the peptide mixtures were analyzed by high resolution MS on a linear ion trap-orbitrap instrument. The vast majority of proteins (>99%) bound equally well to the methylated and nonmethylated peptide and appeared in the mass spectra with equal intensity in the light and heavy form. Proteins interacting in a methylation-dependent manner are present with a higher intensity in the heavy form. This quantitative filter therefore distinguishes specific binders.

When performing this screen for H3K4me3, we identified several known interactors with a significant SILAC ratio. They included BPTF (Figure 1B) and CHD1 (Figure 1C), which have been reported to bind methylated H3K4 via a PHD finger and a double chromodomain, respectively (Wysocka et al. 2006, Li et al., 2006). A number of other novel interactors were identified, which included several PHD finger-containing proteins (see Table S2). Surprisingly, we also identified all TAF subunits of TFIID with highly significant ratios (~30:1), indicating that the TFIID complex specifically binds to trimethylated H3K4 (Figures 1D, 1F, S1–S5, and Table S1). The TATA-binding protein (TBP) showed a SILAC ratio of 4, substantially lower than the ratios of the TFIID TAFs. While still significant, this lower ratio can be explained by the presence of TBP complexes lacking TFIID TAFs, which would bind nonspecifically to bait and control. This is also exemplified by the TAF_I63 (or TAF1B) subunit of SL1 (ratio 0.98, Figure 1F). We verified the preferential interaction between TFIID and H3K4me3 by immunoblotting (Figure 1E).

To investigate the functional consequences of this interaction we performed RNAi experiments against WDR5, which is known to preferentially reduce global levels of the H3K4me3 marks but not of H3K4 me2 and H3K4me1 (Dou et al., 2006; Steward et al., 2006). Figure 2A shows that WDR5 siRNA treatment of U2OS cells indeed resulted in a pronounced reduction of H3K4me3. We examined the mRNA levels of a number of genes to identify promoters sensitive to H3K4me3 loss. As indicated by Figure 2B, WDR5 siRNA treatment reduced the mRNA levels of the HMG-CoA reductase, RPL34, RPS10, and RPL31 genes by about 2-fold. In contrast, fibronectin and the β-actin reference mRNAs were not affected. Analysis of chromatin immunoprecipitation (ChIP) samples by quantitative PCR showed that the WDR5 siRNA reduced TBP association to the HMG-CoA reductase but not to the fibronectin core promoter (Figure 2C). As expected, H3K4me3 modification was reduced on both promoters. An extensive ChIP analysis of TBP and TAF1 binding was performed for the RPL34, RPL31, and RPS10 genes by scanning their 5′ regions using different PCR primer pairs (Figures 2D, 2E and S6). WDR5 siRNA treatment also reduced TBP and TAF1 association to these promoters. TBP and TAF1 ChIP signals were also detected more downstream overlapping with the peak of H3K4me3. This corresponds well with recently published ChIP-chip results for these factors (Bernstein et al., 2005; Heintzman et al., 2007).

Taken together, these results indicate that the entire TFIID complex but not other TBP-containing complexes specifically associates with H3K4me3 peptides in vitro and that the H3K4me3 mark is important for retention of TFIID and the transcriptional activity of a subset of promoters in vivo.

The TAF3-PHD Finger Directly Binds to Trimethylated Histone H3 Lysine 4

Several papers described interactions between PHD fingers containing proteins (including BPTF) and methylated H3K4 or H3K36 peptides (Li et al., 2006; Pena et al., 2006; Shi et al., 2006; Wysocka et al., 2006). Interestingly, the metazoan TAF3 subunit of TFIID contains a PHD finger

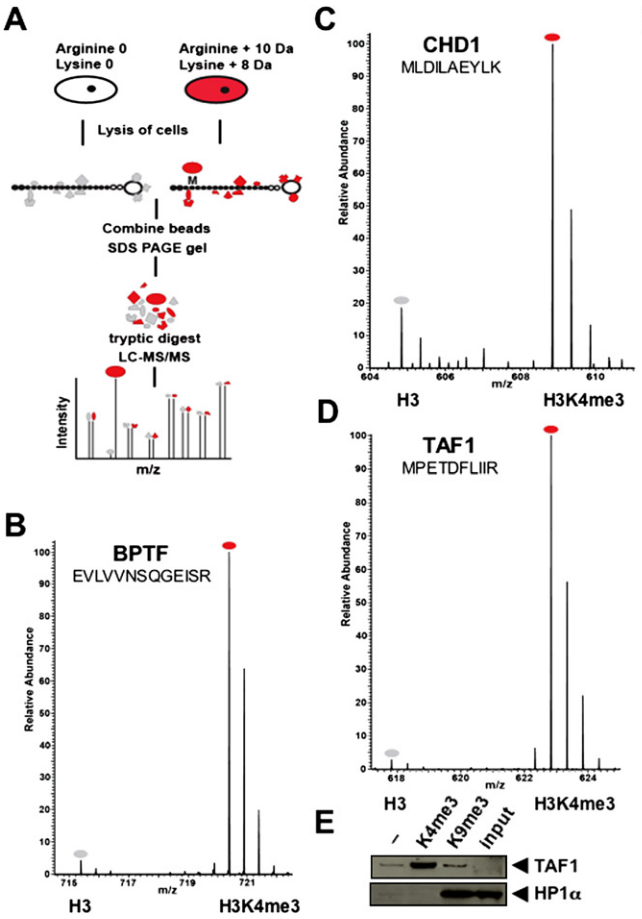

F

Protein*	Quantified peptides	SILAC Ratio	St dev	Mascot score
TAF1	38	38.88	14.90	4544
TAF2	54	31.53	11.34	4950
TAF3	17	31.16	9.64	1357
TAF4	69	35.82	14.11	6092
TAF4B	15	41.16	17.81	1108
TAF5	30	42.68	17.09	3300
TAF6	41	36.50	15.80	3519
TAF7	10	37.32	9.20	808
TAF8	16	37.70	14.30	1643
TAF9	20	32.54	11.36	2044
TAF9b	2	35.75	20.23	197
TAF10	8	34.33	10.30	1089
TAF11	7	44.62	12.48	599
TAF12	8	45.46	17.81	382
TAF13	5	50.4	11	257
TBP	6	3.8	0.4	339
TAF1B (PolI)	20	0.98	0.08	1293

Figure 1. The TFIID Complex Binds to Trimethylated Histone H3 Lysine 4 In Vitro

(A–D) Schematic representation of the SILAC-based histone peptide pull-down approach (Schulze and Mann, 2004). Representative spectra of BPTF (B), CHD1 (C), and TAF1 (D) peptides. The heavy peptide from the SILAC pair is clearly more intense, demonstrating specific binding of these proteins. The gray and red ovals indicate the relative amount of protein binding to the unmodified or H3K4me3 peptide, respectively.

(E) The preferential interaction between TFIID and H3K4me3 was confirmed by pull-downs of nuclear extracts using unmodified (–), H3K4me3 or H3K9me3 peptides. Bound proteins were analyzed by immunoblotting using TAF1 and HP1α antibodies.

(F) Quantification of the interaction of all TFIID-TAFs with H3K4me3 as revealed by SILAC screening. SILAC ratios represent the relative abundance of the heavy to the light peptide indicating specific binding to the H3K4me3 peptide.

at its extreme C terminus (Gangloff et al., 2001; Pointud et al., 2001). Alignment of the PHD fingers of TAF3 and ING2 (Figure 3A) revealed conservation of residues involved in H3K4me3 interaction (Ruthenburg et al., 2007). This suggests that the PHD finger of TAF3 could be critical for the interaction between TFIID and methylated H3K4. To test this hypothesis we generated HeLa cell lines expressing tagged versions of full-length mouse TAF3 or TAF3ΔC80 lacking the C-terminal PHD finger (see Figure S7). Nuclear extracts derived from these cell lines were tested for binding to H3 peptides. Whereas the tagged full-length mTAF3 protein bound specifically to the H3K4me3 peptide (Figure 3B, compare lane 1 and 2), no binding of the tagged mTAF3ΔC80 protein could be observed (lane 3 and 4). The TAF7 subunit of TFIID was also retained by the H3K4me3 peptide, but to a lesser extent in the TAF3ΔC80 extracts (compare lanes 2 and 4). This may be explained by a dominant-negative effect of the TAF3ΔC80 protein, which replaces part of the endogenous TAF3 in the pool of cellular TFIID. Further analysis indicated that the tagged TAF3 proteins are incorporated into TFIID complexes (Figure S7). Thus, TFIID complexes harboring the truncated TAF3ΔC80 subunit are defective for H3K4me3 binding.

To further investigate this we assessed the ability of a GST fusion of the isolated TAF3-PHD finger to bind methylated histone peptides. As shown in Figure 3C, the PHD finger bound very efficiently to methylated H3K4, with a clear preference for H3K4me3, whereas no binding to methylated H3K9 or H3K36 was observed. Based on the sequence alignment we mutated selected residues of the TAF3-PHD finger expected to be involved in H3K4me3 binding (Figure 3A). GST-TAF3 PHD fusions carrying the M882A, D886A, and D890A/W891A mutations were

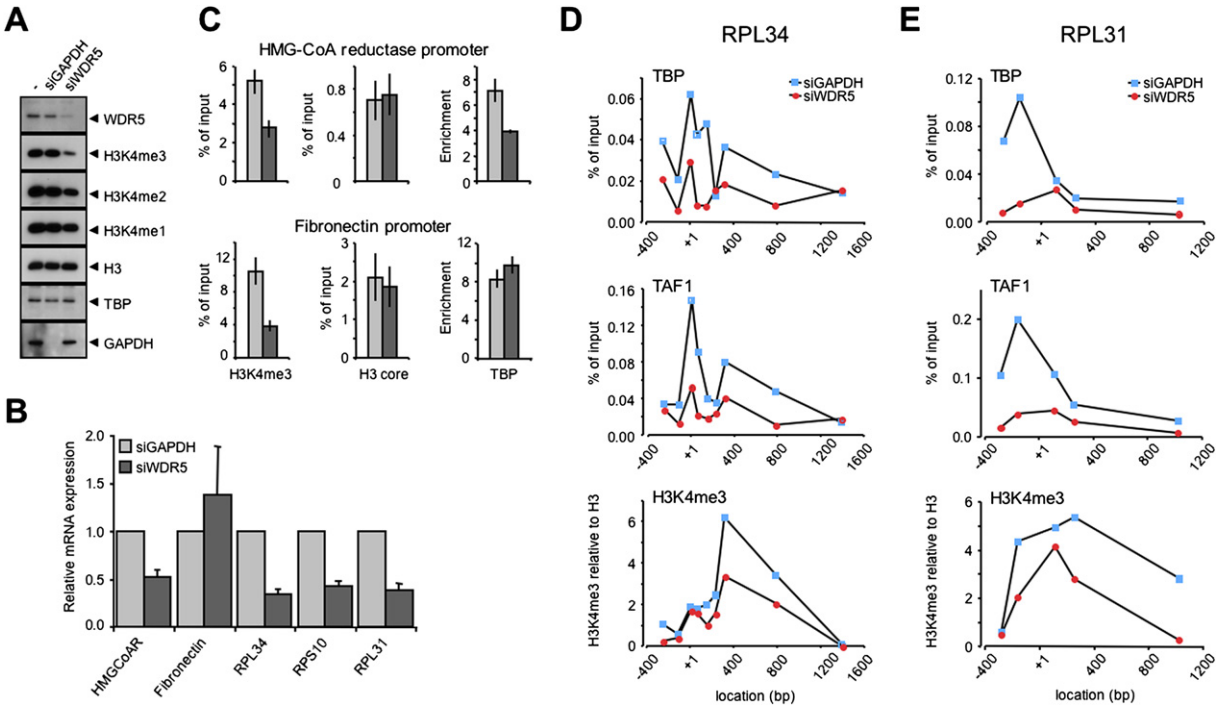

Figure 2. TFIID Occupancy and mRNA Expression Dependence on H3K4me3 In Vivo

(A) Immunoblot analysis on U2OS cell lysates transfected with WDR5 or GAPDH control siRNAs.

(B) Quantitative RT-PCR analysis of siRNA-treated cells. Levels of the different mRNA were normalized on β-actin mRNA levels, which were not affected by the WDR5 knockdown. Error bars indicate standard deviation of three to four biological replicates.

(C) ChIP experiments were performed with siRNA-treated cells to asses H3K4Me3 levels and TBP occupancy on the indicated pol II promoters. An H3 core domain antibody was used as a control. The results are represented as percentage of input for histone antibodies and as folds over background for TBP. Dark gray and light gray bars indicate results with WDR5 or GAPDH control siRNA-transfected cells, respectively. Error bars indicate standard deviation of three biological replicates.

(D and E) A representative ChIP analysis of TAF1, TBP, and H3K4me3 association to the RPL34 and RPL31 loci in siRNA-treated cells. H3K4me3 levels are relative to total H3 levels. TBP and TAF1 levels are represented as percentage of input. Location + 1 indicates the transcription start site.

unable to bind H3K4me3 (Figure 3D). The control A901V mutation did not affect binding efficiency. Previous analysis showed that mutation of equivalent residues in the PHDs of mouse ING2 or human BPTF reduced H3K4me3 binding 20- to 500-fold (Li et al., 2006; Pena et al., 2006). Our mutational analysis underscores the specificity of the interaction and verifies the importance of several residues conserved between PHD fingers (Ruthenburg et al., 2007). To directly compare the affinities between the PHD fingers of TAF3 and ING2 for H3K4me3, we performed a competition experiment under conditions of PHD finger excess over peptide. As shown in Figure 3E, the ING2 and TAF3-PHD finger display similar binding affinities for H3K4me2, whereas the TAF3 PHD clearly has a much higher affinity for H3K4me3 compared to the ING2 PHD. This indicates that the TAF3-PHD finger discriminates strongly between the H3K4me2 and H3K4me3 marks.

To accurately determine the affinities for modified H3 peptides we performed equilibrium binding assays with the TAF3-PHD finger using tryptophan fluorescence. Using the same methodology, the dissociation constant of the ING2 PHD for H3K4me3 was determined to be 1.5 μM (Pena et al., 2006). In our experiments and as expected from Figure 3E, binding of the TAF3 PHD to the H3K4me3 peptide was much stronger with a dissociation constant of 0.16 μM (Figure 3F). The higher affinity of the TAF3 PHD compared to ING2 PHD most likely relates to subtle differences in the geometry of the aromatic cage involved in binding of the trimethyl lysine (I869 and W891 in mTAF3 versus Y215 and W238 in mING2). Structural analysis of the PHD finger of TAF3 will provide further insight into this. Taken together, H3 peptide-binding assays identified the PHD finger of TAF3 as necessary and sufficient for recognition of the H3K4me3 mark.

The TAF3 PHD Finger Binds to Nucleosomes Containing Trimethylated Histone H3K4

The experiments described so far indicate that the TFIID complex binds via the PHD of TAF3 with a high selectivity to histone H3K4me3 peptides. To extend these observations we isolated nucleosomes from HeLa cells and various yeast strains (Figure 4A and data not shown) to investigate whether the TAF3 PHD finger is able to recognize the H3K4me3 mark in native chromatin. As shown in Figures 4B and 4C, immunoblotting with modification-specific antibodies revealed that the bound nucleosomes were

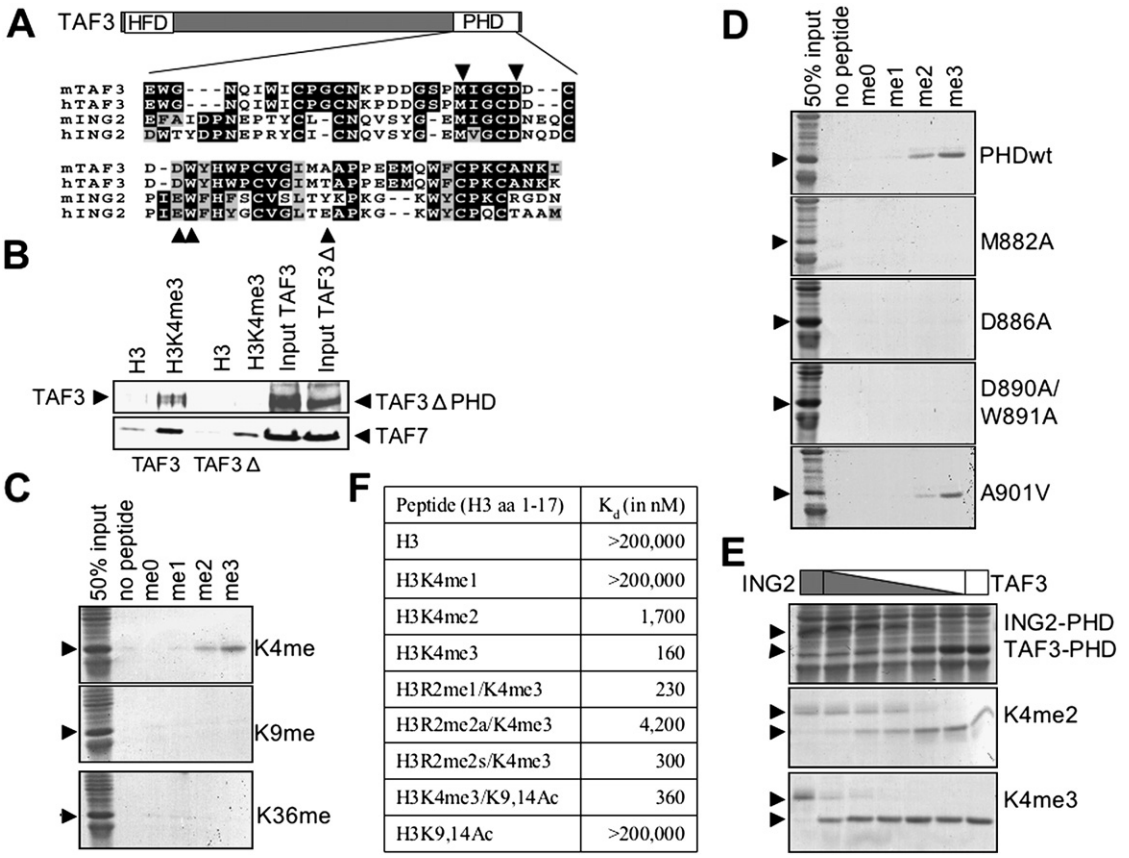

F

Peptide (H3 aa 1-17)	K_d (in nM)
H3	>200,000
H3K4me1	>200,000
H3K4me2	1,700
H3K4me3	160
H3R2me1/K4me3	230
H3R2me2a/K4me3	4,200
H3R2me2s/K4me3	300
H3K4me3/K9,14Ac	360
H3K9,14Ac	>200,000

Figure 3. The Isolated PHD Finger of TAF3 Binds with High Specificity to H3K4me3

(A) Domain representation of the TAF3 subunit of TFIID indicating the N-terminal histone-fold domain (residues 9–82) and C-terminal PHD finger (residues 870–914). Alignment of the PHDs of mouse TAF3 (862–918), human TAF3 (860–914), mouse ING2 (205–266), and human ING2 (352–406). Arrowheads indicate positions of mutants tested in (D).

(B) Nuclear extracts derived from HeLa stable cell lines expressing either full-length HA-tagged TAF3 or a mutant lacking the PHD finger were used for pull-downs using the indicated peptides. Immunoblotting was performed for the presence of endogenous TAF7 and exogenous TAF3 proteins in the pull-down eluates. Please note that the TAF7 signal in the H3K4me3 pull-down of the TAF3ΔPHD lysate most likely corresponds to TFIID complexes containing endogenous TAF3.

(C) Bacterial lysates containing GST-mTAF3 (857–924) were incubated with streptavidin-beads coated with the indicated H3 peptides. Bound proteins were analyzed by Coomassie staining. Arrowheads indicate position of the GST-fusion protein.

(D) Wild-type and mutant TAF3-PHD proteins (as indicated to the right) were analyzed as in (C) for binding to K4-methylated peptides as indicated above.

(E) Competitive binding of GST-fusion proteins of the PHD of mouse ING2 and TAF3 to H3 peptides indicated to the right. The top panel shows 2.5% of the input. The percentage of TAF3-PHD lysate is 0%, 5%, 10%, 20%, 50%, 80%, and 100% (from left to right) of the total used for binding.

(F) Dissociation constants of TAF3-PHD binding to H3 peptides (residues 1–17) carrying the indicated modifications as determined by tryptophan fluorescence.

enriched for H3K4me3 and contained only low levels of H3K4me2 or H3K4me1. DNA analysis of bound yeast nucleosomes indicated retention of mono-, di-, and trinucleosomes (Figure 4C). In agreement with the peptide pull-down, the two PHD mutants D886A and D890A/W891A were unable to bind yeast nucleosomes, indicating the specificity of binding. To address the importance of the H3K4 trimethylation mark for the binding, we isolated nucleosomes from yeast strains carrying deletions in genes responsible for different histone methylation marks (Figure 4D). The *SET1*, *SET2*, and *DOT1* genes encode histone methyltransferase (HMT) enzymes for H3K4, H3K36, and H3K79, respectively (Martin and Zhang, 2005). *SPP1* encodes a subunit of the Set1p/COMPASS HMT complex and has been shown to be important for efficient H3K4 trimethylation, but not di- or monomethylation of H3K4 (Dehe et al., 2006; Schneider et al., 2005). As predicted the TAF3 PHD finger binds nucleosomes from *set2Δ* and *dot1Δ* strains indicating that neither H3K36 nor H3K79 methylation is required for binding to nucleosomes (Figure 4E). However, in the *set1Δ* and *spp1Δ* strains, in which H3K4 (tri-)methylation is abolished, nucleosome binding was lost. These results indicate that the TAF3 PHD finger binds specifically to native H3K4me3-marked nucleosomes.

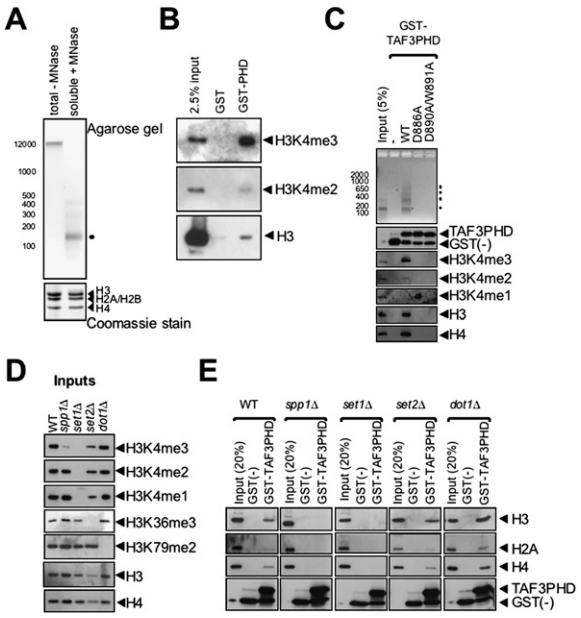

Figure 4. The PHD Finger of TAF3 Specifically Interacts with H3K4 Trimethylated Native Nucleosomes

(A) Soluble native mononucleosomes from HeLa cells were analyzed by agarose-gel electrophoresis for DNA content and SDS-PAGE followed by Coomassie staining for histones.

(B) Beads were coated with GST or GST-TAF3PHD and incubated with native HeLa nucleosomes. Bound material was analyzed by immunoblot analysis using modification-specific antibodies.

(C) Beads were coated with GST or GST-TAF3PHD (WT or mutants) and incubated with native yeast nucleosomes. Precipitated material was analyzed as in (A) and (B).

(D) Nucleosomal preparations isolated from various mutant yeast strains were subjected to immunoblot analysis to determine the H3 methylation status.

(E) The indicated nucleosomal preparations were subjected to GST pull-down and analysis as in (B).

Asymmetric Dimethylation of H3R2 Selectively Inhibits Recognition of the H3K4me3 Mark by TFIID and TAF3 PHD

The structure of the WDR5 protein bound to an N-terminal peptide of histone H3 indicated that methylation of H3R2 negatively affected WDR5 binding (for review, see Sims and Reinberg, 2006). Furthermore, in yeast, asymmetric dimethylation of H3R2 inhibits the binding of the PHD finger protein SPP1 to methylated H3K4 (A. Kirmizis and T. Kouzarides, personal communication). To investigate a potential inhibitory effect of H3R2 methylation on the H3K4me3 binding of PHD finger proteins we compared several differentially methylated histone H3 peptides. This revealed that asymmetric dimethylation of H3R2 drastically reduces the binding of the TAF3 PHD to H3K4me3, whereas this effect was not observed for the ING2 or BPTF PHD (Figure 5A). This was confirmed in a competition experiment (Figure 5B), which revealed that the ING2 and TAF3-PHD finger have a similar affinity for the doubly methylated peptide (R2me2a/K4me3). In agreement with the GST-PHD pull-downs, H3R2me2a results in a 25-fold lower binding constant of the H3K4me3 modified peptide, whereas H3R2me2s and H3R2me1 display little effect (Figure 3F). Together, these analyses indicate that asymmetric dimethylation of H3R2 counters the high affinity of the PHD finger of TAF3 but not of ING2 and BPTF for the H3K4me3 mark.

To further investigate the effect of asymmetric dimethylation of H3R2 on the binding of the TFIID complex to trimethylated H3K4, we extended our quantitative proteomics approach to simultaneously assay three different histone modification marks (H3 unmodified, H3K4me3, and H3R2me2a/K4me3) with three differentially SILAC-labeled extracts. This assay allows direct visualization of potential agonistic and antagonistic effects of modifications. The spectra in Figure 5C show that H3K4me3 binding by the TFIID complex (exemplified by its subunits TAF1 and TAF7) is compromised by the H3R2me2a modification. Importantly, binding of the BPTF protein was not affected (Figure 5C), indicating that the effect is specific to the TAF PHD finger. Together, these experiments reveal crosstalk between different histone modifications at the level of TAF3-PHD and TFIID-complex binding.

Acetylation of H3K9 and H3K14 Is Agonistic to H3K4me3

Similar to trimethylation of H3K4, acetylation of the adjacent lysines (K9 and K14) is generally associated with active promoters (Millar and Grunstein, 2006). The TAF1 subunit of metazoan TFIID contains an acetyl-lysine binding activity residing in its double bromodomain (Jacobson et al., 2000). We compared the combined effects of acetylation and methylation of the histone H3 tail on TFIID and BPTF binding using the SILAC triple pull-down approach. As shown in Figure 6A, K9 and K14 acetylation had a minor effect on retention of TAF1 (and other TFIID TAFs, data not shown). BPTF, which contains both a PHD and a bromodomain, showed a similar binding behavior. The presence of the H3K4me3 mark in addition to H3K9,14Ac strongly augmented retention of TAF1 (and the other TFIID TAFs) and of BPTF (additional increase in SILAC ratio ~10-fold). In contrast, the BAF180/polybromo subunit of the human BAF chromatin-remodeling complex, which contains multiple bromodomains but no PHD finger (Nicolas and Goodwin, 1996), bound equally strong to the H3K9,14Ac and H3K4me3/K9,14Ac peptides (SILAC ratio > 8-fold over the unmodified peptide; right panel in Figure 6A).

We next tested whether acetylation enhances the binding of TFIID to H3K4me3 in an experiment comparing unmodified H3 with H3K4me3 and H3K4me3/K9,14Ac peptides. As shown in Figure 6B, both TAF1 and BPTF binding to H3K4me3 was markedly increased by acetylation at H3K9 and H3K14. As expected we failed to observe preferential binding of BAF180/polybromo to the H3K4me3 peptide, whereas the protein was retained efficiently by the H3 peptide containing both acetylation and methylation marks. Affinity measurements and H3 peptide pull-downs also indicated that acetylation on K9 and K14

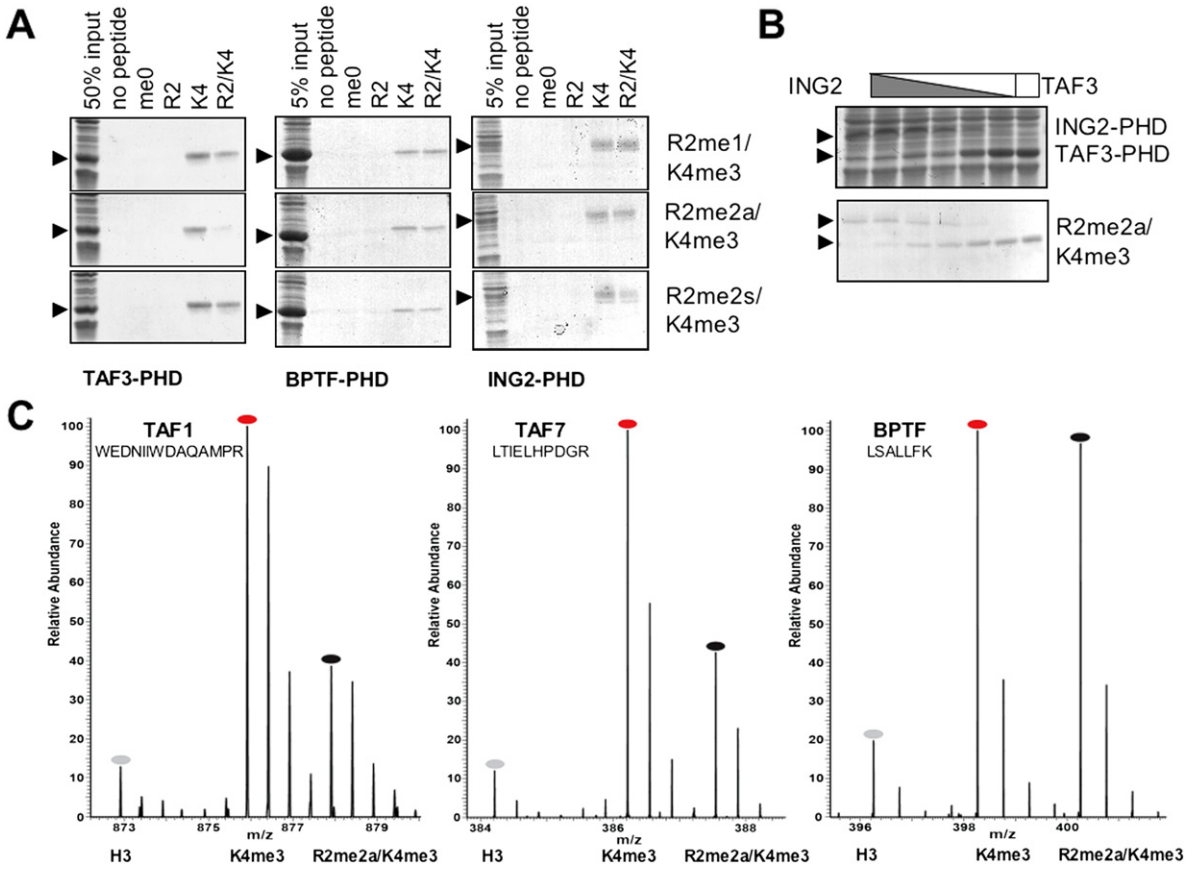

Figure 5. H3R2me2a Selectively Inhibits Binding of TFIID to H3K4me3

(A) Pull-downs using the indicated peptides were performed as described in Figure 3.

(B) Competition experiment between GST-TAF3-PHD and GST-ING2-PHD as described in Figure 3E using the H3K4me3 and H3R2me2a/K4me3 peptides.

(C) A triple SILAC peptide pull-down was performed using an unmodified (H3), an H3K4me3, and an H3K4me3/H3R2me2a doubly methylated peptide. The spectra show the relative binding of TAF1 (left), TAF7 (middle), and BPTF (right) to these three peptides as indicated. The gray ovals represent the relative protein binding to the unmodified H3 peptide, the red ovals represent the binding to the H3K4me3 peptide, and the black ovals represent the binding to the doubly modified H3K4me3/H3R2me2a peptide. Note that the ratio for the TAF subunits is somewhat lower compared to those shown in Figure 1, which is caused by a variation in washing efficiency.

had little effect on the affinity of the isolated PHD of TAF3 for the H3K4me3 peptide (Figures 3F and S8).

Collectively, these experiments indicate that both for TFIID and BPTF the PHD-mediated interaction to H3 tails is augmented by K9 and K14 acetylation. We propose that the combinatorial effects of H3K4me3 binding via TAF3 and H3K9,14Ac binding via TAF1 results in a strong interaction between TFIID and transcriptionally active promoters.

TAF3 Can Act as a Transcriptional Coactivator in a PHD Finger-Dependent Manner

To obtain further support for the hypothesis that TAF3 acts as a transcriptional cofactor by recognizing H3K4me3 we examined the effect of siRNA-mediated knockdown of TAF3 on the expression of the WDR5-dependent genes. Quantitative RT-PCR analysis indicated that similar to the WDR5 siRNA, treatment of U2OS cells with TAF3 siRNA reduced the mRNA levels for HMG-CoA reductase, RPL34, RPL31, and RPS10 but not for fibronectin (Figure 7A). Next, we employed a luciferase reporter assay in which the Ash2L subunit of Set1/MLL histone methyltransferase complexes was targeted to a test promoter as a Gal4 DNA-binding domain fusion. The evolutionary conserved Ash2L protein has been shown to be essential for efficient H3K4 di- and trimethylation and incorporates into the MLL1 complex via direct interaction with the Rbbp5 subunit (Dou et al., 2006; Steward et al., 2006). We reasoned that this could provide a functional assay for TAF3-dependent activation of transcription. Expression of the Gal4-Ash2L resulted in activation of promoter activity in human U2OS osteosarcoma cells. Coexpression of wild-type TAF3 greatly enhanced Gal4-Ash2L-mediated activation in a Gal4 binding site-dependent manner (Figure 7B). In contrast, the

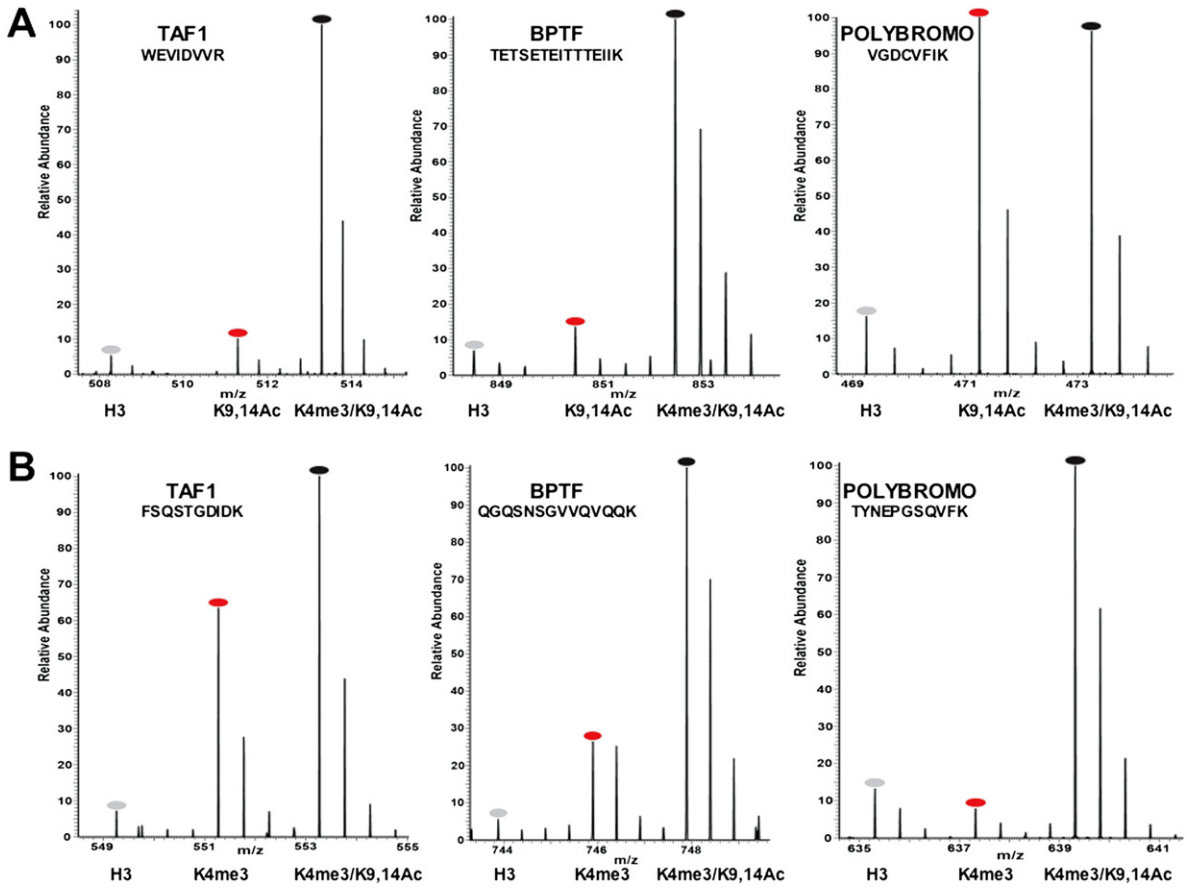

Figure 6. Acetylation of H3K9 and K14 Acts Agonistically with H3K4me3 to Anchor TFIID on the Histone H3 Tail

(A and B) Triple SILAC pull-downs were performed using peptides as indicated to investigate the relative contribution of H3K4me3 and H3K9,14Ac on TFIID binding.

PHD finger point mutants M882A and D886A were not efficient in coactivation. Immunoblotting of transfected cell lysates indicated a similar expression of the transfected proteins (Figure 7C). Together, these experiments indicate that TAF3 can act as a transcriptional cofactor and support the model of Figure 7D in which methylation of histone H3K4 provides a binding site for the TFIID complex, resulting in enhanced recruitment or stability of the RNA polymerase II preinitiation complex.

DISCUSSION

In this study we provide evidence that trimethylation of lysine 4 of histone H3 serves as a high-affinity binding site for mammalian TFIID and that the PHD finger of the TAF3 subunit mediates this interaction. We investigated crosstalk of H3K4me3 with other modifications and found an inhibitory effect of H3R2me2a on TFIID binding, whereas H3K9,14Ac enhanced TFIID binding. This correlates well with active transcription and the genome-wide distributions of these histone marks and TAF1 (Bernstein et al., 2005; Heintzman et al., 2007; Millar and Grunstein, 2006).

Function of the H3K4me3 Mark as a Docking Site

Methylation of H3K4 is a universal histone mark in the eukaryotic kingdom, and it has been studied in most detail in yeast cells. Trimethylation of H3K4 has been proposed to link transcription initiation to elongation and mRNA processing (Krogan et al., 2003; Morillon et al., 2005). Strikingly, yeast TAF3 lacks a PHD finger, indicating that this domain has been acquired relatively late in evolution (Gangloff et al., 2001). Several observations suggest that H3K4me3 may serve new or additional roles in higher eukaryotes. First, the H3K4me3 mark remains limited to the first ~1 kb of a gene (Bernstein et al., 2005; Heintzman et al., 2007). Accordingly, the H3K4me3 modification is much less abundant in human nucleosomes compared to yeast (Figure 4) (Taverna et al., 2007). Second, whereas the yeast genome encodes 18 PHDs in 14 different proteins, the PHD is much more prevalent in higher eukaryotes genomes (38 PHDs in flies and ~150 in humans) (Bienz, 2006).

The observation that eight of the 18 yeast PHDs are able to bind methylated H3K4 (Shi et al., 2007) raises the question how many of the human PHD fingers can bind

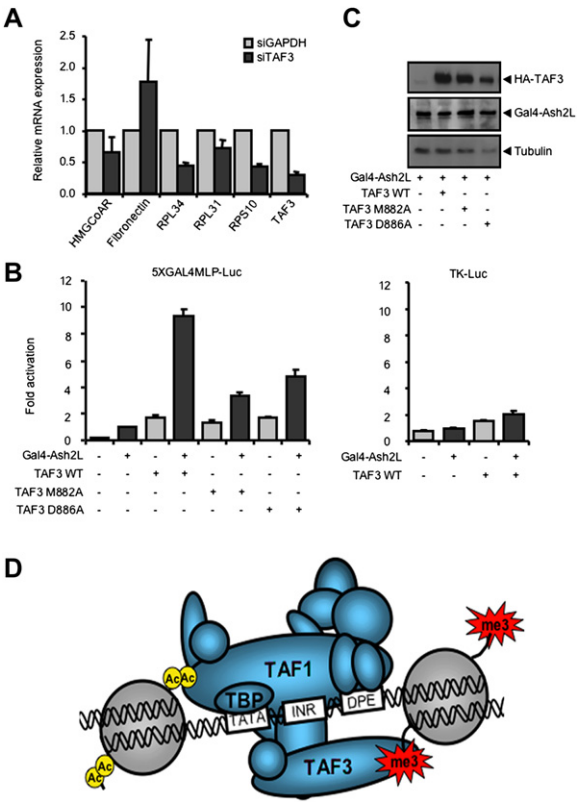

Figure 7. Transcriptional Activation by TAF3

(A) Quantitative RT-PCR analysis of siRNA-treated cells. Levels of the different mRNA were normalized on β-actin mRNA levels, which were not affected by the TAF3 knockdown. Error bars indicate standard deviation of two biological replicates. Knockdown of TAF3 expression was assessed at the mRNA level as appropriate TAF3 antibodies are not available.

(B) U2OS cells were transiently transfected in triplicates (errors bars indicate standard deviations) with the 5XGal4MLP-Luc reporter plasmid and pMT2-HA empty vector or pMT2-HA expression plasmids for the wild-type TAF3 or its M882A and D886A mutants in the presence or absence of Gal4-Ash2L as indicated below the panels. The experiment shown in the left panel is representative of three biological replicates. In the right panel U2OS cells were transfected in duplicates with the luciferase reporter construct TK-Luc lacking Gal4-binding sites and in the presence or absence of Gal4-Ash2L and TAF3 plasmids as indicated. The graphs represent the fold activation relative to the transfection with Gal4-Ash2L alone.

(C) U2OS cells were transfected with the indicated constructs and analyzed for protein expression by SDS-PAGE and immunoblotting. The tubulin-loading control indicates that less protein was loaded in the TAF3-D886A lane.

(D) Model depicting the different chromatin- and DNA-mediated interactions involved in anchoring the TFIID complex to the core promoter. In red stars the H3K4me3 methylation mark recognized by the PHD domain of TAF3 is indicated and in yellow the (di-)acetylation mark interacting with the double-bromo domain of TAF1. In addition, DNA-sequence specific interactions of TBP with the TATA box, of TAF1/2 with the initiator element, and of TAF6/9 with the downstream promoter element (DPE) are shown.

methylated H3K4. Our proteomic screen of HeLa cell extracts identifies seven PHD finger-containing proteins specifically binding H3K4me3 (Table S2). Importantly, multiple complexes with opposing activities are now known to compete for H3K4me3 binding: repression via ING2/Sin3A (Shi et al., 2006), chromatin remodeling via BPTF/NURF (Wysocka et al., 2006), and gene activation by TFIID (this paper). The finding that the TAF3 PHD has a 10- to 20-fold higher affinity for H3K4me3 than the PHDs of ING2 and BPTF indicates that via TAF3 TFIID can effectively compete with these (opposing) activities.

Relevance of TFIID Binding to H3K4me3 for Transcription

Current models for the function of H3K4 methylation are largely derived from yeast studies. They are supported by an elegant in vitro study using human proteins, which suggests that the H3K4me3 appears after the basal transcription machinery has assembled on the promoter (Pavri et al., 2006). In this scenario TAF3-dependent anchoring of TFIID could stimulate subsequent rounds of transcription. Other observations suggest the possibility that in human cells H3K4 methylation can act at the promoter activation step since gene-specific transcription factors like activated nuclear receptors and CREB can interact directly with subunits of MLL complexes (Dreijerink et al., 2006; Ernst et al., 2001; Garcia-Bassets et al., 2007; Lee et al., 2006). We found that loss of the H3K4me3 mark resulted in a reduced TFIID association and transcriptional activity of certain promoters, which also depend on TAF3 expression. In addition, transient transfections (Figure 7B) show that expression of TAF3 enhances the transcriptional stimulation by the Ash2L subunit of H3K4 methylase complexes. Taken together, this suggests that TAF3-mediated binding of TFIID to H3K4me3-marked nucleosomes can serve either to anchor TFIID to activated promoters or to recruit TFIID during promoter activation.

Recruitment of TFIID to gene promoters is governed both by its interaction with gene-specific transcription factors and coactivators and by the "quality" of the core promoter (Albright and Tjian, 2000). Whereas TBP binds with high affinity ($K_d \sim 1$ nM) to a canonical TATA box, several other TFIID subunits can recognize core promoter elements like the INR (TAF1/2), DCE (TAF1), (DPE TAF6/9), and MTE (TAF1) with lower affinities (Juven-Gershon et al., 2006; Lee et al., 2005). Only a subset of mammalian promoters contains a classical TATA box, which stresses the importance of the other DNA elements. Our study indicates that histone modifications of the core promoter should also be taken into consideration (Figure 7D). A previous study of the yeast *PHO5* promoter showed that nucleosome sliding can induce dependence on acetylation of the H4 tail and a bromodomain-containing protein (Martinez-Campa et al., 2004). We propose that H3K4 trimethylation plays an important role in defining a core promoter as it creates a binding site for the TAF3 subunit of TFIID. Strikingly, the fibronectin and β-actin promoters contain a TATA box and are insensitive to loss of

H3K4me3 or TAF3. In contrast to the H3K4me3/TAF3-dependent HMG-CoA reductase promoter, the RPL34, RPL31, and RPS10 promoters all lack a canonical TATA box. It is tempting to speculate that the TAF3-H3K4me3 interaction may be most important for promoters lacking canonical core promoter DNA elements. Large-scale identification of TAF3-dependent promoters would allow testing of these models and determine the relevance of the H3K4me3-TFIID interactions for their transcription.

Crosstalk between Different Histone Modifications

An important aspect of the "histone code" hypothesis is that the modifications act in combination (Strahl and Allis, 2000). Our analysis provides two new examples of combinatorial control for binding to methylated H3K4. For the isolated TAF3 PHD we observed that asymmetric methylation of H3R2 inhibits H3K4me3 binding of TAF3 but not of ING2 or BPTF. The H3R2me2a modification also inhibits binding of the TFIID complex. Genome-wide analysis indicated the co-occurrence of the H3K4me3 and H3K9,14Ac marks in human cells (Bernstein et al., 2005; Heintzman et al., 2007). Our proteomic analysis clearly shows that TFIID binding to H3K4me3 is enhanced by coincident H3K9,14Ac modification. Most likely, this effect is mediated by the double bromodomain of TAF1. Whereas this domain preferentially binds to diacetylated H4 tails, it also binds to singly acetylated tails with low affinity ($K_d \sim 40\ \mu M$) (Jacobson et al., 2000). Consistently, the TFIID complex shows little enrichment with H3K9,14Ac compared to the nonacetylated peptide in the SILAC experiments. The dominance of H3K4me3 in TFIID binding can be readily explained by the higher affinity of the TAF3 PHD for this mark.

In conclusion, we have employed high-accuracy quantitative proteomics using the SILAC technology to discover a direct connection between histone trimethylation and the basal transcription machinery. One striking observation described in this work is the remarkable affinity of the TAF3 PHD finger for H3K4me3 and the cooperative effect with acetylation of H3K9,K14. These facts and given the general presence of H3K4me3 on active promoters as well as the broad importance of the TFIID complex for eukaryotic transcription suggest that the interaction between TFIID and H3K4me3 is highly relevant for the activation of genes in mammalian cells. An interesting question that remains is whether the interaction between H3K4me3 and TFIID is secondary following promoter recruitment or whether the interaction can serve as a primary recruitment signal for TFIID to promoters. Our findings direct future experiments to resolve these two possibilities.

EXPERIMENTAL PROCEDURES

Protein Extraction and Peptide Pull-Downs

HeLaS3 cells were grown in suspension in the presence of normal lysine and arginine or heavy versions of these (Isotec). Nuclear extracts were prepared as described (Dignam et al., 1983). Histone peptides containing the N-terminal 17 amino acids of the histone H3 followed by two glycines and a biotinylated lysine were synthesized using the Fmoc strategy as described (Schulze and Mann, 2004). Peptides were immobilized on Dynabeads MyOne Streptavidin C1 (Dynal) and subsequently incubated with 350 μg of nuclear extract (diluted to 0.6 mg/ml) in binding buffer (150 mM NaCl, 50 mM Tris-HCl at pH8.0, 1% NP40, 1 mM DTT, and complete protease inhibitors -EDTA [Roche]) for 2 hr at 4°C in a rotation wheel. Beads were washed five times with 1 ml of binding buffer containing 400 mM NaCl and finally twice with 1 ml of binding buffer. Beads from both pull-downs (unmodified and modified peptide) were subsequently pooled, and bound proteins were eluted and analyzed on 4%–12% gradient gels (Invitrogen) by colloidal blue staining (Invitrogen). For immunoblotting, antibodies against TAF1 (Upstate, #05-500), and HP1α (Upstate, #07-346) were used.

Mass Spectrometry of Proteins

After trypsin digestion of gel slices peptides were extracted, desalted using StageTips (Rappsilber et al., 2003), and analyzed using a nano-HPLC Agilent 1100 nanoflow system connected online to an linear trap quadropole (LTQ)-Orbitrap mass spectrometer (Thermo Fisher, Bremen). The mass spectrometer was operated in the data-dependent mode to automatically switch between MS and MS^2. The instrument was operated with "lock-mass option" as recently described (Olsen et al., 2005). Survey spectra were acquired with 60,000 resolution in the orbitrap, while acquiring up to five tandem mass spectra in the LTQ part of the instrument. Fragment spectra were searched using the MASCOT software program (Matrix Science, UK). MSQuant (http://msquant.sourceforge.net/) was used to verify and quantify the resulting peptide pairs. The median ratio of all ratios between 2 and 0.5 was used to determine the standard deviation from the 1:1 ratio. The protein ratios for all TAFs were more than ten standard deviations away from this median value. Each pull-down experiment was performed at least three times with independent batches of extracts, with similar results.

Mammalian Cell Culture, Chromatin Immunoprecipitation (ChIP), mRNA Analyses, and Transient Reporter Assays

Human U2OS osteosarcoma cells were transfected with siRNAs (Dharmacon) according to the manufacturer's instructions. Formaldehyde-crosslinked chromatin samples were prepared as described (Bernstein et al., 2005; Denissov et al., 2007; Heintzman et al., 2007). The ChIP samples were analyzed by qPCR, and mRNA levels were determined by quantative RT-PCR as described (Dreijerink et al., 2006). PCR primers and siRNA sequences are available upon request.

For luciferase assays U2OS cells were transfected in duplicates or triplicates (as indicated) by using FuGENE 6 (Roche Applied Science). Firefly reporter luciferase constructs 5XGal4MLP-Luc or TK-Luc (100 ng) were cotransfected with 50 ng TK promoter-driven *Renilla* luciferase plasmid for differences in transfection efficiency and 250 ng pMT2-HA-mTAF3 constructs. Cell lysates were prepared 38 hr after transfection, and luciferase activity was determined using the Dual-Luciferase Reporter Assay System (Promega).

To analyze levels of transfected proteins, U2OS cells were plated on 6-well tissue culture plates and transfected with 500 ng Gal4-Ash2L expression plasmid and 500 ng mTAF3 wild-type (WT) or mutant plasmids. Total cell lysates were analyzed by immunoblotting using anti-HA (3F10) or Gal4-DBD (RK5C1, Santa Cruz, CA) antibodies and enhanced chemiluminescence (ECL, Amersham Biosciences).

H3 Peptide- and Nucleosome-Binding Experiments

H3 peptides immobilized on streptavidin-conjugated dynabeads were incubated with crude bacterial GST-TAF-PHD induced lysates in binding buffer (50 mM Tris-HCl at pH 8.0, 150 mM NaCl, 0.1% NP40, 10 μM $ZnCl_2$, 1 mM DTT, and protease inhibitors) for 2–3 hr at 4°C. Following extensive washing bound proteins were eluted and analyzed by SDS-PAGE and Coomassie brilliant blue R-250 (Biorad).

For nucleosome-binding experiments glutathione-agarose beads were coated with bacterial lysates containing GST or GST-TAF3PHD (WT or mutant). Mononucleosomes were mixed with GST-coated

agarose beads and incubated overnight at 4°C in H3-binding buffer. Beads were washed five times with H3-binding buffer. Twenty-five percent was used for extraction of DNA using the QiaQuick PCR purification kit (QIAGEN) and resolved on a 1.5% agarose gel. The remainder was prepared for immunoblot analysis. Antibodies specific for H3, H3K4me1, H3K4me2, H3K4me3, and H4 (ab1791, ab8895, ab7766, ab8580, and ab31827) were obtained from Abcam. Antibodies against H3K36me3 (GTX80647), H3K79me2, and H2A (#07–366 and #07–146) were obtained from GeneTex, Inc. and Upstate Biotechnology, respectively. GST-fusion proteins were detected with a GST antibody conjugated to HRP (Amersham, 27–4588).

H3 Peptide Affinity Measurements

The TAF3-PHD(857–924) was expressed as a GST-fusion protein and purified essentially as described (Dominguez et al., 2004). The resulting protein was further purified by anion exchange chromatography and estimated to be > 95% pure by Coomassie staining. For K_d measurements the TAF3-PHD protein was diluted to 100 nM for H3K4me3, H3R2me1/K4me3, H3R2me2s/K4me3, to 200 nM for H3K4me3/K9,14Ac, and to 1 μM for H3R2me2a/K4me3, H3K9,14Ac, H3K4me2, H3K4me1, and unmodified peptides in H3-binding buffer plus 0.001% Tween-20. Tryptophane fluorescence was determined using a Varian Cary Eclipse fluorescence spectrophotometer using 1.2 ml cuvettes with stirring. The excitation wavelength was 280 nm and slit width 2.5 nm. Emission was determined in the range of 335–355 nm with a 10 nm (for 100 nM PHD), 5 nm (for 200 nM PHD), or a 2.5 nm slit width (for 1 μM PHD) with an averaging time of 5 s and 2 nm data interval. Each measurement was repeated at least three times with two different batches of H3 peptide.

Supplemental Data

Supplemental Data include eight figures, two tables, Supplemental Experimental Procedures, and Supplemental References and can be found with this article online at http://www.cell.com/cgi/content/full/131/1/58/DC1/.

ACKNOWLEDGMENTS

We gratefully acknowledge Drs. Davidson, Tora, Gozani, and Patel for providing plasmids, Dr. Stewart for various yeast strains, Dr. W. Herr for WDR5 antibody, and Dr. Rehmann for help with the tryptophan fluorescence measurements. We are indebted to Dr. Lüscher for communication of unpublished results and providing the Gal4-Ash2L plasmid. We also thank Drs. van Ingen, Wienk, and Boelens for designing the TAF3-PHD mutants. We also thank Dr. Kraus, Dr. Rehmann, and members of the Stunnenberg, Mann, and Timmers labs for stimulating discussions.

This work was supported by grants to the Timmers lab from the European Union (STREP LSHG-CT-2004-502950) and the Netherlands Proteomics Centre. Furthermore, the work in the Mann and Stunnenberg labs is supported by HEROIC, an Integrated Project funded by the European Union under the 6th Framework Programme (LSHG-CT-2005-018883). The research of M.V. is supported by a TALENT grant of the Netherlands Organization for Scientific Research (NWO) and by a fellowship of the Dutch Cancer Society (KWF/NKB).

Received: February 19, 2007
Revised: May 9, 2007
Accepted: August 15, 2007
Published online: September 20, 2007

REFERENCES

Aebersold, R., and Mann, M. (2003). Mass spectrometry-based proteomics. Nature *422*, 198–207.

Albright, S.R., and Tjian, R. (2000). TAFs revisited: more data reveal new twists and confirm old ideas. Gene *242*, 1–13.

Bernstein, B.E., Kamal, M., Lindblad-Toh, K., Bekiranov, S., Bailey, D.K., Huebert, D.J., McMahon, S., Karlsson, E.K., Kulbokas, E.J., 3rd, Gingeras, T.R., et al. (2005). Genomic maps and comparative analysis of histone modifications in human and mouse. Cell *120*, 169–181.

Bienz, M. (2006). The PHD finger, a nuclear protein-interaction domain. Trends Biochem. Sci. *31*, 35–40.

Carrozza, M.J., Utley, R.T., Workman, J.L., and Cote, J. (2003). The diverse functions of histone acetyltransferase complexes. Trends Genet. *19*, 321–329.

Dehe, P.M., Dichtl, B., Schaft, D., Roguev, A., Pamblanco, M., Lebrun, R., Rodriguez-Gil, A., Mkandawire, M., Landsberg, K., Shevchenko, A., et al. (2006). Protein interactions within the Set1 complex and their roles in the regulation of histone 3 lysine 4 methylation. J. Biol. Chem. *281*, 35404–35412.

Denissov, S., van Driel, M., Voit, R., Hekkelman, M., Hulsen, T., Hernandez, N., Grummt, I., Wehrens, R., and Stunnenberg, H. (2007). Identification of novel functional TBP-binding sites and general factor repertoires. EMBO J. *26*, 944–954.

Dignam, J.D., Lebovitz, R.M., and Roeder, R.G. (1983). Accurate transcription initiation by RNA polymerase II in a soluble extract from isolated mammalian nuclei. Nucleic Acids Res. *11*, 1475–1489.

Dominguez, C., Bonvin, A.M., Winkler, G.S., van Schaik, F.M., Timmers, H.T., and Boelens, R. (2004). Structural model of the UbcH5B/CNOT4 complex revealed by combining NMR, mutagenesis, and docking approaches. Structure *12*, 633–644.

Dou, Y., Milne, T.A., Ruthenburg, A.J., Lee, S., Lee, J.W., Verdine, G.L., Allis, C.D., and Roeder, R.G. (2006). Regulation of MLL1 H3K4 methyltransferase activity by its core components. Nat. Struct. Mol. Biol. *13*, 713–719.

Dreijerink, K.M., Mulder, K.W., Winkler, G.S., Hoppener, J.W., Lips, C.J., and Timmers, H.T. (2006). Menin links estrogen receptor activation to histone H3K4 trimethylation. Cancer Res. *66*, 4929–4935.

Ernst, P., Wang, J., Huang, M., Goodman, R.H., and Korsmeyer, S.J. (2001). MLL and CREB bind cooperatively to the nuclear coactivator CREB-binding protein. Mol. Cell. Biol. *21*, 2249–2258.

Gangloff, Y.G., Pointud, J.C., Thuault, S., Carre, L., Romier, C., Muratoglu, S., Brand, M., Tora, L., Couderc, J.L., and Davidson, I. (2001). The TFIID components human TAF(II)140 and Drosophila BIP2 (TAF(II)155) are novel metazoan homologues of yeast TAF(II)47 containing a histone fold and a PHD finger. Mol. Cell. Biol. *21*, 5109–5121.

Garcia-Bassets, I., Kwon, Y.S., Telese, F., Prefontaine, G.G., Hutt, K.R., Cheng, C.S., Ju, B.G., Ohgi, K.A., Wang, J., Escoubet-Lozach, L., et al. (2007). Histone methylation-dependent mechanisms impose ligand dependency for gene activation by nuclear receptors. Cell *128*, 505–518.

Heintzman, N.D., Stuart, R.K., Hon, G., Fu, Y., Ching, C.W., Hawkins, R.D., Barrera, L.O., Van Calcar, S., Qu, C., Ching, K.A., et al. (2007). Distinct and predictive chromatin signatures of transcriptional promoters and enhancers in the human genome. Nat. Genet. *39*, 311–318.

Jacobson, R.H., Ladurner, A.G., King, D.S., and Tjian, R. (2000). Structure and function of a human TAFII250 double bromodomain module. Science *288*, 1422–1425.

Jenuwein, T., and Allis, C.D. (2001). Translating the histone code. Science *293*, 1074–1080.

Juven-Gershon, T., Cheng, S., and Kadonaga, J.T. (2006). Rational design of a super core promoter that enhances gene expression. Nat. Methods *3*, 917–922.

Kim, J., Daniel, J., Espejo, A., Lake, A., Krishna, M., Xia, L., Zhang, Y., and Bedford, M.T. (2006). Tudor, MBT and chromo domains gauge the degree of lysine methylation. EMBO Rep. *7*, 397–403.

Krogan, N.J., Dover, J., Wood, A., Schneider, J., Heidt, J., Boateng, M.A., Dean, K., Ryan, O.W., Golshani, A., Johnston, M., et al. (2003). The Paf1 complex is required for histone H3 methylation by COMPASS and Dot1p: linking transcriptional elongation to histone methylation. Mol. Cell *11*, 721–729.

Lee, D.H., Gershenzon, N., Gupta, M., Ioshikhes, I.P., Reinberg, D., and Lewis, B.A. (2005). Functional characterization of core promoter elements: the downstream core element is recognized by TAF1. Mol. Cell. Biol. *25*, 9674–9686.

Lee, S., Lee, D.K., Dou, Y., Lee, J., Lee, B., Kwak, E., Kong, Y.Y., Lee, S.K., Roeder, R.G., and Lee, J.W. (2006). Coactivator as a target gene specificity determinant for histone H3 lysine 4 methyltransferases. Proc. Natl. Acad. Sci. USA *103*, 15392–15397.

Leurent, C., Sanders, S.L., Demeny, M.A., Garbett, K.A., Ruhlmann, C., Weil, P.A., Tora, L., and Schultz, P. (2004). Mapping key functional sites within yeast TFIID. EMBO J. *23*, 719–727.

Li, H., Ilin, S., Wang, W., Duncan, E.M., Wysocka, J., Allis, C.D., and Patel, D.J. (2006). Molecular basis for site-specific read-out of histone H3K4me3 by the BPTF PHD finger of NURF. Nature *442*, 91–95.

Mann, M. (2006). Functional and quantitative proteomics using SILAC. Nat. Rev. Mol. Cell Biol. *7*, 952–958.

Margueron, R., Trojer, P., and Reinberg, D. (2005). The key to development: interpreting the histone code? Curr. Opin. Genet. Dev. *15*, 163–176.

Martin, C., and Zhang, Y. (2005). The diverse functions of histone lysine methylation. Nat. Rev. Mol. Cell Biol. *6*, 838–849.

Martinez-Campa, C., Politis, P., Moreau, J.L., Kent, N., Goodall, J., Mellor, J., and Goding, C.R. (2004). Precise nucleosome positioning and the TATA box dictate requirements for the histone H4 tail and the bromodomain factor Bdf1. Mol. Cell *15*, 69–81.

Millar, C.B., and Grunstein, M. (2006). Genome-wide patterns of histone modifications in yeast. Nat. Rev. Mol. Cell Biol. *7*, 657–666.

Morillon, A., Karabetsou, N., Nair, A., and Mellor, J. (2005). Dynamic lysine methylation on histone H3 defines the regulatory phase of gene transcription. Mol. Cell *18*, 723–734.

Nicolas, R.H., and Goodwin, G.H. (1996). Molecular cloning of polybromo, a nuclear protein containing multiple domains including five bromodomains, a truncated HMG-box, and two repeats of a novel domain. Gene *175*, 233–240.

Olsen, J.V., de Godoy, L.M., Li, G., Macek, B., Mortensen, P., Pesch, R., Makarov, A., Lange, O., Horning, S., and Mann, M. (2005). Parts per Million Mass Accuracy on an Orbitrap Mass Spectrometer via Lock Mass Injection into a C-trap. Mol. Cell. Proteomics *4*, 2010–2021.

Olsen, J.V., Blagoev, B., Gnad, F., Macek, B., Kumar, C., Mortensen, P., and Mann, M. (2006). Global, in vivo, and site-specific phosphorylation dynamics in signaling networks. Cell *127*, 635–648.

Ong, S.E., and Mann, M. (2005). Mass spectrometry-based proteomics turns quantitative. Nat. Chem. Biol. *1*, 252–262.

Pavri, R., Zhu, B., Li, G., Trojer, P., Mandal, S., Shilatifard, A., and Reinberg, D. (2006). Histone H2B monoubiquitination functions cooperatively with FACT to regulate elongation by RNA polymerase II. Cell *125*, 703–717.

Pena, P.V., Davrazou, F., Shi, X., Walter, K.L., Verkhusha, V.V., Gozani, O., Zhao, R., and Kutateladze, T.G. (2006). Molecular mechanism of histone H3K4me3 recognition by plant homeodomain of ING2. Nature *442*, 100–103.

Pointud, J.C., Larsson, J., Dastugue, B., and Couderc, J.L. (2001). The BTB/POZ domain of the regulatory proteins Bric a brac 1 (BAB1) and Bric a brac 2 (BAB2) interacts with the novel Drosophila TAF(II) factor BIP2/dTAF(II)155. Dev. Biol. *237*, 368–380.

Rappsilber, J., Ishihama, Y., and Mann, M. (2003). Stop and go extraction tips for matrix-assisted laser desorption/ionization, nanoelectrospray, and LC/MS sample pretreatment in proteomics. Anal. Chem. *75*, 663–670.

Ruthenburg, A.J., Allis, C.D., and Wysocka, J. (2007). Methylation of lysine 4 on histone H3: intricacy of writing and reading a single epigenetic mark. Mol. Cell *25*, 15–30.

Santos-Rosa, H., Schneider, R., Bannister, A.J., Sherriff, J., Bernstein, B.E., Emre, N.C., Schreiber, S.L., Mellor, J., and Kouzarides, T. (2002). Active genes are tri-methylated at K4 of histone H3. Nature *419*, 407–411.

Schneider, J., Wood, A., Lee, J.S., Schuster, R., Dueker, J., Maguire, C., Swanson, S.K., Florens, L., Washburn, M.P., and Shilatifard, A. (2005). Molecular regulation of histone H3 trimethylation by COMPASS and the regulation of gene expression. Mol. Cell *19*, 849–856.

Schulze, W.X., and Mann, M. (2004). A novel proteomic screen for peptide-protein interactions. J. Biol. Chem. *279*, 10756–10764.

Shi, X., Hong, T., Walter, K.L., Ewalt, M., Michishita, E., Hung, T., Carney, D., Pena, P., Lan, F., Kaadige, M.R., et al. (2006). ING2 PHD domain links histone H3 lysine 4 methylation to active gene repression. Nature *442*, 96–99.

Shi, X., Kachirskaia, I., Walter, K.L., Kuo, J.H., Lake, A., Davrazou, F., Chan, S.M., Martin, D.G., Fingerman, I.M., Briggs, S.D., et al. (2007). Proteome-wide analysis in Saccharomyces cerevisiae identifies several PHD fingers as novel direct and selective binding modules of histone H3 methylated at either lysine 4 or lysine 36. J. Biol. Chem. *282*, 2450–2455.

Sims, R.J., 3rd, and Reinberg, D. (2006). Histone H3 Lys 4 methylation: caught in a bind? Genes Dev. *20*, 2779–2786.

Steward, M.M., Lee, J.S., O'Donovan, A., Wyatt, M., Bernstein, B.E., and Shilatifard, A. (2006). Molecular regulation of H3K4 trimethylation by ASH2L, a shared subunit of MLL complexes. Nat. Struct. Mol. Biol. *13*, 852–854.

Strahl, B.D., and Allis, C.D. (2000). The language of covalent histone modifications. Nature *403*, 41–45.

Taverna, S.D., Ueberheide, B.M., Liu, Y., Tackett, A.J., Diaz, R.L., Shabanowitz, J., Chait, B.T., Hunt, D.F., and Allis, C.D. (2007). Long-distance combinatorial linkage between methylation and acetylation on histone H3 N termini. Proc. Natl. Acad. Sci. USA *104*, 2086–2091.

Tora, L. (2002). A unified nomenclature for TATA box binding protein (TBP)-associated factors (TAFs) involved in RNA polymerase II transcription. Genes Dev. *16*, 673–675.

Torres-Padilla, M.E., Parfitt, D.E., Kouzarides, T., and Zernicka-Goetz, M. (2007). Histone arginine methylation regulates pluripotency in the early mouse embryo. Nature *445*, 214–218.

Wysocka, J., Swigut, T., Xiao, H., Milne, T.A., Kwon, S.Y., Landry, J., Kauer, M., Tackett, A.J., Chait, B.T., Badenhorst, P., et al. (2006). A PHD finger of NURF couples histone H3 lysine 4 trimethylation with chromatin remodelling. Nature *442*, 86–90.